WOOD RESEARCH
59 (2): 2014
303-312

FIBRE AND ADHESIVE BRIDGING AT GLUE JOINTS IN EUROPEAN BEECH WOOD

Samuel Ammann, Peter Niemz
Institute For Building Materials, Department of Civil, Environmental and Geomatic Engineering
Eth Zürich
Zürich
Switzerland

(Received December 2013)

ABSTRACT

The fibre and adhesive bridging at glue joints in European beech (*Fagus sylvatica* L.) was investigated under standard atmospheric conditions (65 % relative humidity, 20°C). Solid wood samples were taken as reference. Three different types of adhesives were used for bonding: Melamine urea formaldehyde resin (MUF), phenol resorcinol formaldehyde resin (PRF) and one-component polyurethane (PUR). A compact sample geometry was used to assure only little displacement at initial rupture, leaving as many bridges as possible intact. The load was applied displacement controlled in pure opening mode. The loading rate was varied between 5 to 3125 $\mu m \cdot min^{-1}$ to highlight possible creep and rate effects. The results of the MUF, PRF and solid wood samples however show no dependency on the loading rate. Only the rupture energy of the PUR samples increases with increasing loading rates, from around 350 to 450 $N \cdot m^{-1}$. This range is completely congruent with literature values. MUF, like PRF, tend to 100 % wood failure, but while MUF exhibits the same behaviour as solid wood, PRF performs worse.

KEYWORDS: Fibre bridging, delamination, adhesive, European beech.

INTRODUCTION

Structural hardwood elements have gained more popularity in civil engineering during the last decade. Shapes are getting more complex and high ratios of slenderness are favoured. Consequently the demands on structural elements are rising and thus the use of hardwood becomes more appealing. Common hardwoods like beech (*Fagus sylvatica* L.) have higher strength parameters and moduli of elasticity than the more frequently used spruce wood (*Picea abies* KARST.) (Niemz 1993). However, beech also has higher shrinkage and swelling coefficients than spruce (Wagenführ 2007), which together with the high mechanical properties leads to increased internal stresses and increases the risk of delamination at glue joints. In addition, wood adhesives are mostly developed for use with softwoods and might not be totally suitable for use with hardwoods. Therefore the basic behaviour of glue joints in hardwoods has to be studied from different perspectives to reliably estimate the load bearing capacities of adhesively bonded structural hardwood elements.

Several approaches were pursued to overcome this problem. Sonderegger et al. (2010) for example analysed the influence of different adhesives on the diffusion processes and highlighted moisture concentrations at glue joints, which potentially increase the risk of delamination. Clauß et al. (2011) studied the formulation of PUR adhesives and the influence of different components on the bond performance, and Schmidt et al. (2010) wanted to optimise the manufacturing process of hardwood elements to fulfil the required standards. Glue joints were also investigated on the micro scale: Hass et al. (2010, 2012) studied the pore space of beech wood and the resulting penetration behaviour of adhesives into it, and the adhesion of different adhesives onto the wood cell wall was measured by the use of nanoindentation (Ammann et al. 2014; Obersriebnig et al. 2012).

Fibre bridging is a well-known phenomenon and ubiquitous in wood fracture (Stanzl-Tschegg et al. 1995; Vasic and Smith 2002; Keunecke et al. 2007), but it is normally simply regarded as part of a propagating crack and has never been studied on its own. Therefore, an attempt was made here to separate the bridging from the fracture itself to determine absolute values of bridge spans and energy consumption of their rupture. Requirements from the fracture mechanical standpoint were of lower priority, since only the behaviour after initial failure was of interest.

MATERIAL AND METHODS

Sample preparation

All experiments were performed under standard atmospheric conditions (65 % relative humidity, 20°C). Before sample preparation the wood was stored at standard atmosphere until moisture equilibrium was reached.

European beech (*Fagus sylvatica* L., density: 645 ± 10 $kg \cdot m^{-3}$, moisture content: 14 %) was used as adherend and bonded with three different types of adhesives:

- One-component polyurethane (1C PUR) HB S 709 provided by Purbond AG, Sempach-Station, Switzerland,
- melamine urea formaldehyde resin (MUF) Kauramin (glue 683, hardener 688) provided by BASF SE, Ludwigshafen, Germany,
- phenol resorcinol formaldehyde resin (PRF) Aerodux (glue 185 RL, hardener HP 155) provided by Bolleter Composites AG, Arbon, Switzerland.

All bonding parameters were strictly adopted from the manufacturers' guidelines.

The beech wood boards with an approximate size of 7 × 40 cm were planed to a thickness of 3 mm. The adhesives were applied within 24 h after planing. Before the adherends were joined, 35 mm wide silicon paper strips (thickness: 35 μm) were placed directly in the adhesive (see Fig. 1). The silicon paper has two characteristics: It impedes the bonding at its specific location, and stresses are concentrated at its edges, serving as almost crack-like failure initiation in the glue joint (ISO 25217, 2009).

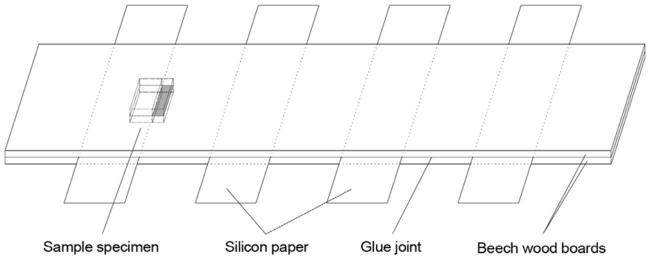

Fig. 1: Bonded boards (sketch).

The bonded boards were conditioned for a minimum of 7 days before the final specimens were cut out. One sample was taken from each side of each silicon paper strip, as denoted in Fig. 1. In the last step the sample face opposite the silicon paper was concave shaped (see Fig. 2). This step was necessary to reduce the stress concentration along the edges, which in preliminary tests led to problems in the fixation.

The final samples contain 2 cm^2 (10 × 20 mm) silicon paper and 1 cm^2 (5 × 20 mm) actual bonded area with a sample height of 6 mm. The exact geometry is shown in Fig. 2 and is based on the findings of Olejniczak and Gustafsson (1994). The compact shape is necessary for an initial failure at only little displacement, leaving the fibre and adhesive bridges intact.

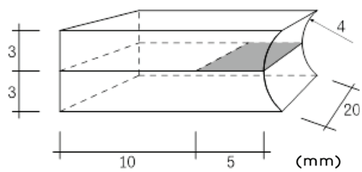

Fig. 2: Sample geometry. The actual bonded area is marked grey.

Solid wood (SW) samples were shaped the same way as the bonded samples. Instead of silicon paper the initial crack was defined using a scroll saw and a microtome blade for the final crack tip.

Test setup

All experiments were conducted on a Zwick/Roell Z010 testing machine with a 10 kN load cell. Aluminium T-sections with a flange and web thickness of 4 mm were mounted in the machine clamps and aligned for flat, parallel surfaces perpendicular to the loading direction (see Fig. 3). In a first step the sample was attached to the lower T-section with a cyanoacrylate adhesive. While curing of the cyanoacrylate, the machine was used as pressing device with approximately 90 % of the original adhesive bonding pressure to prevent damage at the glue joint. After 1 hour the machine was opened, cyanoacrylate was applied on the upper sample surface and then the machine was closed again for 1 hour. After curing of the cyanoacrylate the pressure was slowly reduced. When the point of zero pressure was reached, the actual measurement started. Five loading rates were used: 5, 25, 125, 625 and 3125 $\mu m \cdot min^{-1}$, resulting in complete separation of the adherends within a few seconds up to approximately 3 hours. These increments shall highlight possible creep and rate effects on the gathered results.

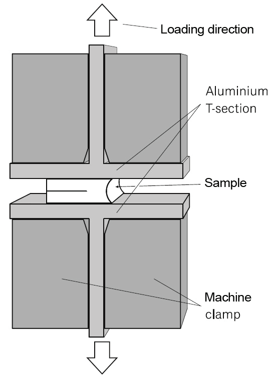

Fig. 3: Test setup with mounted sample.

Data evaluation

With the given sample geometry and test setup, failure will occur immediately after a critical stress level is reached at the silicon paper edge in the adhesive or at the predefined crack in the solid wood, respectively. The initial rupture takes place after very little displacement, leaving intact as many fibre and adhesive bridges as possible. The abrupt failure allows classifying the results into two states: intact state with no notable damage and ruptured state including bridging until complete separation of the adherends, as noted in Fig. 4 (see also Stanzl-Tschegg et al. 1995).

The failure type, cohesive or adhesive, was estimated according to EN 302-1 (2013) and denoted as wood failure percentage (WFP).

Besides the maximum displacement, u_{max}, that the bridges can span and the failure type, the energy needed to overcome the bridging is also of interest. The total specific energy, E_{tot}, invested to separate the adherends corresponds to the integral of the force (F) over displacement (u) divided by the fractured area (A) and can be separated into the initial rupture energy E_I (corresponding to the light grey area in Fig. 4) and the bridging rupture energy E_B (corresponding to the dark grey area in Fig. 4):

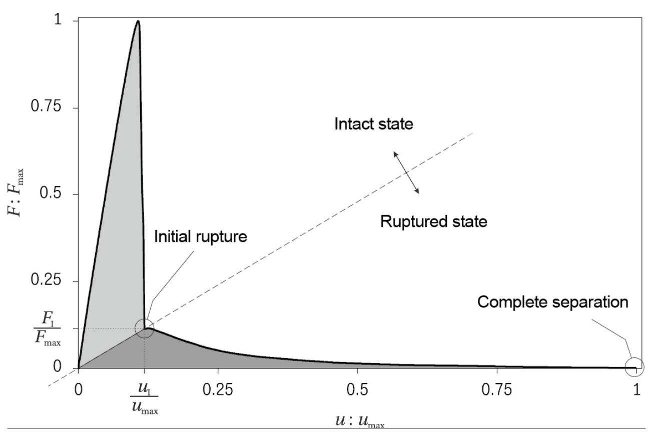

Fig. 4: Representative normalised load displacement curve.

$$E_{tot} = E_I + E_B = \frac{1}{A} \cdot \int_0^{u_{max}} F\mathrm{d}u \quad (1)$$

$$E_I = \frac{1}{A} \cdot \int_0^{u_I} F\mathrm{d}u - \frac{F_I u_I}{2A} \quad (2)$$

$$E_B = \frac{1}{A} \cdot \int_{u_I}^{u_{max}} F\mathrm{d}u + \frac{F_I u_I}{2A} \quad (3)$$

where: F_I and u_I - the force and the displacement, respectively, at the time of the initial rupture.

E_{tot} - cannot be equalised with the specific fracture energy G_f, commonly found in literature covering fracture mechanics. The compact sample geometry interferes with the stress field before initial rupture, leading to complex stress situations around the crack tip. However, the bridging effect benefits from the compact geometry, with also short bridges staying intact after initial rupture. Additionally, E_{tot} can still be compared within the sample size, and E_B is not affected.

Statistical significances of the gathered results are evaluated according to DIN 53804-1 (2002) with a level of significance of 5 %.

RESULTS AND DISCUSSION

Influence of loading rate

Most of the results show no significant dependency on the loading rate. Therefore, where no influence was measurable, the results were grouped together by the adhesive type.

No significant influence of the loading rate was measurable for the MUF, PRF and SW specimens. The maximum stress, σ_{max}, at rupture increases by trend with increasing loading rates, but with lack of significance.

In PUR specimens, the total specific energy, E_{tot}, increases at higher loading rates, as shown in Fig. 5. The bridging energy however is not affected, with a mean value of 82 ± 10 $N \cdot m^{-1}$ (see also Fig. 7). Also the extent of the bridging energy compared to the overall energy is not significantly affected, being in the range of 21 ± 2 %.

In Fig. 5 the grey area indicates the specific fracture energy of PUR as found in the literature, extending the range 300 to 500 $N \cdot m^{-1}$ (Veigel et al. 2012; Serrano 2000). As this figure shows, the results found here are completely congruent with the literature values, even though no proper conditions for fracture mechanic testing are given here. Thus the rupture behaviour of PUR glue joints mostly depends on the adhesive and cohesive behaviour of the adhesive, rather than on the adherend.

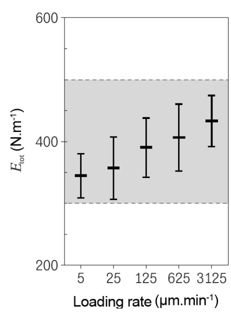

Fig. 5: Mean values and confidence intervals of E_{tot} of the PUR bonded samples for different loading rates.

Gagliano (2001) came to similar results concerning the effect of loading rate on adhesively bonded wood. Despite using a viscoelastic polyvinyl acetate latex as adhesive, he was not able to measure a significant influence of the loading rate on his results.

Wood failure percentage

All the MUF bonded specimens have a WFP of 100 %. For the PUR bonded specimens, the WFP is 0 %. The results for PRF specimens are more variable (see Fig. 6). Approximately half of the specimens exhibit the same performance as the MUF specimens, with a mean WFP of 85 %.

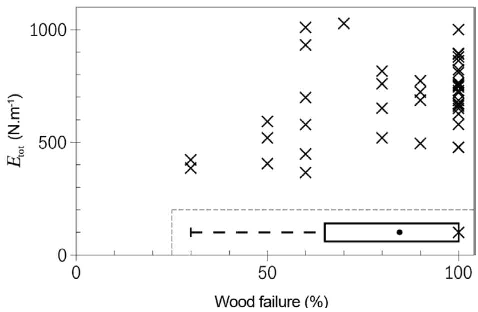

Fig. 6: WFP of PRF bonded specimens. The black dot in the boxplot indicates the mean value and the cross indicates the median.

However, a WFP as low as 30 % was also observed. These two specimens did not fail in adhesion, but failed cohesively inside the adhesive. This behaviour could be caused by poor bonding. The WFP of the PRF specimens correlate with the total rupture energy (Fig. 6), but not with the loading rate.

Bridge span and rupture energy

The mean values of the energies and the bridge spans with their respective confidence intervals are shown in Fig. 7. This figure clearly shows that MUF bonded samples act like the solid wood samples. Their maximum bridge spans are identical and the bridging energies do not

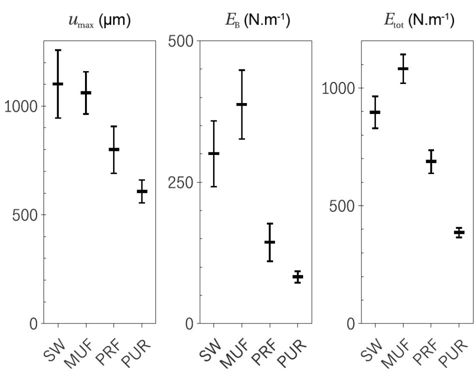

Fig. 7: Mean values and confidence intervals of the maximum displacements u_{max} that the bridges can span, the specific energies E_B needed to separate the bridges, and the total specific energies E_{tot} invested to rupture the samples.

vary significantly. The increased total energy can be explained with the higher fracture toughness of MUF compared to beech wood, as noted by Watson et al. (2013). These results correspond with a WFP of 100 %. Hence, properly produced MUF glue joints in beech wood are tougher than the sole wood (under standard atmosphere) and therefore do not influence potential failure in such elements.

PRF in contrast, having a similar behaviour to MUF regarding the WFP, shows significant shorter bridge spans and lower rupture energies than solid wood. The mean bridge span of PRF bonded specimens corresponds to 75 %, and the bridging energy to 50 % of the solid wood specimens. The maximum stresses at initial rupture however, are equal. Subsequently, it can be concluded that, even when the failure occurs in the adherend, the PRF influences the failure mechanism. The weakest zone of such glue joints therefore is not the bond line, but the adjacent adherend in contact with the PRF. Konnerth et al. (2007) conclude that PRF adhesive, or components of it, penetrate the wood cell wall, and Adamopoulos et al. (2012) measured a penetration depth of PRF into beech wood of 240 µm. Accordingly it seems plausible that the penetration into the cell wall reduces the strength parameters of the wood up to 240 µm on both sides of the glue joint, resulting in a failure in the adherend close to the bond line. This zone corresponds to the adherend subsurface according to adhesive bond model of Marra (1992).

In civil engineering it is generally premised that a bonding has to be tougher than the joined elements. This basic principle is also adapted in standards for structural wood products, such as EN 386 (2001) or ASTM D2559-12a (2012). There, a certain amount of wood failure is demanded, assuming that wood failure represents the strength of the adherend. However, the findings herein reveal an ambiguity in the interpretation of the WFP.

CONCLUSIONS

The experiments carried out in this study allow the following conclusions:

The peculiarities of fibre bridges at brittle glue joints are not affected by variable loading rates.

- PUR with beech adherends fails in adhesion. The energy needed to overcome this adhesion depends on the loading rate.
- MUF and PRF glue joints both fail in the adherend, but:
- MUF glue joints act like the solid wood,
- PRF glue joints are weaker than the solid wood.

However, one has to keep in mind that these findings are not universally valid and have to be seen in the right context, as already stated by Custódio et al. (2009).

ACKNOWLEDGMENT

This research was carried out at ETH Zürich and funded through the National Research Programme NRP 66 of the Swiss National Science Foundation. The idea and principle for this research arose during discussions with professor P.J. Gustafsson at Lund University.

REFERENCES

1. Adamopoulos, S., Bastani, A., Gascón-Garrido, P., Militz, H., Mai, C., 2012: Adhesive bonding of beech wood modified with a phenol formaldehyde compound. European Journal of Wood and Wood Products 70(6): 897-901.
2. Ammann, S., Obersriebnig, M., Konnerth, J., Gindl-Altmutter, W., Niemz, P., 2014: Comparative adhesion analysis at glue joints in european beech and norway spruce wood by means of nano indentation. International Journal of Adhesion and Adhesives 50: 45-49.
3. ASTM D2559-12a, 2012: Standard specification for adhesives for bonded structural wood products for use under exterior exposure conditions.
4. Clauß, S., Gabriel, J., Karbach, A., Matner, M., Niemz, P., 2011: Influence of the adhesive formulation on the mechanical properties and bonding performance of polyurethane prepolymers. Holzforschung 65(6): 835-844.
5. Custódio, J., Broughton, J., Cruz, H., 2009: A review of factors influencing the durability of structural bonded timber joints. International Journal of Adhesion and Adhesives 29(2): 173-185.
6. DIN 53804-1, 2002: Statistical evaluation – Part 1: Continuous characteristics.
7. EN 302-1, 2013: Adhesives for load-bearing timber structures – Test methods – Part 1: Determination of longitudinal tensile shear strength.
8. EN 386, 2001: Glued laminated timber – Performance requirements and minimum production requirements.
9. Gagliano, J.M., 2001: An improved method for the fracture cleavage testing of adhesively-bonded wood. Master's thesis, Virginia Polytechnic Institute and State University.
10. Hass, P., Wittel, F.K., McDonald, S.A., Marone, F., Stampanoni, M., Herrmann, H.J., Niemz, P., 2010: Pore space analysis of beech wood: The vessel network. Holzforschung 64(5): 639-644.
11. Hass, P., Wittel, F., Mendoza, M., Herrmann, H.J., Niemz, P., 2012: Adhesive penetration in beech wood: Experiments. Wood Science and Technology 46(1-3): 243-256.
12. ISO 25217, 2009: Adhesives–determination of the mode 1 adhesive fracture energy of structural adhesive joints using double cantilever beam and tapered double cantilever beam specimens.
13. Keunecke, D., Stanzl-Tschegg, S., Niemz, P., 2007: Fracture characterisation of yew and spruce in the radial-tangential and tangential-radial crack propagation system by a micro wedge splitting test. Holzforschung 61(5): 582-588.
14. Konnerth, J., Harper, D., Lee, S.-W., Rials, T.G., Gindl, W., 2007: Adhesive penetration of wood cell walls investigated by scanning thermal microscopy (SThM). Holzforschung 62(1): 91-98.
15. Marra, A.A., 1992: Technology of wood bonding: Principles in practice. Van Nostrand Reinhold, New York, 454 pp. ISBN 0442007973.
16. Niemz, P., 1993: Physik des Holzes und der Holzwerkstoffe. DRW, Leinfelden-Echterdingen, ISBN 3871813249.
17. Obersriebnig, M., Veigel, S., Gindl-Altmutter, W., Konnerth, J., 2012: Determination of adhesive energy at the wood cell-wall/UF interface by nanoindentation (NI). Holzforschung 66(6): 781-787.
18. Olejniczak, P., Gustafsson, P.J., 1994: Rate effect in tangential tension fracture softening performance. COST 508 – Wood mechanics. Workshop on service life assessment of wooden structures. Espoo, Finland, Session 2 - Fatigue and fracture. Pp 137-148.

19. Schmidt, M., Glos, P., Wegener, G., 2010: Verklebung von Buchenholz für tragende Holzbauteile. European Journal of Wood and Wood Products 68(1): 43-57.
20. Serrano, E., 2000: Adhesive joints in timber engineering. Modelling and testing of fracture properties. PhD thesis, Lund University, Sweden.
21. Sonderegger, W., Hering, S., Mannes, D., Vontobel, P., Lehmann, E., Niemz, P., 2010: Quantitative determination of bound water diffusion in multilayer boards by means of neutron imaging. European Journal of Wood and Wood Products 68(3): 341-350.
22. Stanzl-Tschegg, S.E., Tan, D.M., Tschegg, E.K., 1995: New splitting method for wood fracture characterization. Wood Science and Technology 29(1): 31-50.
23. Vasic, S., Smith, I., 2002: Bridging crack model for fracture of spruce. Engineering Fracture Mechanics 69(6): 745-760.
24. Veigel, S., Follrich, J., Gindl-Altmutter, W., Müller, U., 2012: Comparison of fracture energy testing by means of double cantilever beam-(DCB)-specimens and lap joint testing method for the characterization of adhesively bonded wood. European Journal of Wood and Wood Products 70(1-3): 3-10.
25. Wagenführ, R., 2007: Holzatlas. Fachbuchverlag, Leipzig, 6th edition, ISBN 3446406492.
26. Watson, P., Clauß, S., Ammann, S., Niemz, P., 2013: Determination of fracture properties of adhesive joints under mechanical stresses. Wood Research 58(1): 43-56.

Samuel Ammann, Peter Niemz
Institute For Building Materials
Department of Civil, Environmental and Geomatic Engineering
Eth Zürich, Hif E 27
Stefano-Franscini-Platz 3
8093 Zürich
Switzerland
Phone: +41-44-633-71-56
Corresponding author: ammanns@ethz.ch